ACADEMIC PRESS

Available online at www.sciencedirect.com
SCIENCE DIRECT®

Journal of Catalysis 216 (2003) 288–297

JOURNAL OF CATALYSIS

www.elsevier.com/locate/jcat

Transition metal anion exchanged layered double hydroxides as a bioinspired model of vanadium bromoperoxidase

Bert F. Sels, Dirk E. De Vos, Mieke Buntinx, and Pierre A. Jacobs *

Centre for Surface Chemistry and Catalysis, Katholieke Universiteit Leuven, Kasteelpark Arenberg 23, 3001, Heverlee, Belgium

Received 9 July 2002; revised 9 September 2002; accepted 17 September 2002

On the occasion of the fortieth anniversary of the Journal of Catalysis

Abstract

Tungstate-exchanged layered double hydroxides (LDHs) and V-bromoperoxidase enzymes perform oxidative brominations in a highly similar way: first H_2O_2 binds on the metal to form a peroxometal complex; next the peroxometal oxidizes Br^- to "Br^+"; this electrophilic "Br^+" halogenates an organic compound, or oxidizes a second H_2O_2 molecule to form excited state singlet oxygen. Full evidence for this similarity is given, based on spectroscopic observation of peroxotungstate and $^1O_2$ and on identification of the organic bromination products. In comparison with the homogeneous oxometallates, or with heterogeneous Ti-catalysts, the bioinspired LDH–WO_4^{2-} catalyst displays much higher rates of Br^- oxidation; this rate enhancement is explained. The activity of LDH–WO_4^{2-} can be enhanced by changing the elemental composition of the octahedral layer of the LDH structure. Since LDH–WO_4^{2-} is stable toward leaching and high H_2O_2 concentrations, it is a practical catalyst for oxidative bromination.

Keywords: Biomimetic catalysis; Bromination; Haloperoxidase; Tungsten; Layered double hydroxide; Hydrogen peroxide

1. Introduction

In the catalytic preparation of fine chemicals, the biocatalytic and chemocatalytic approaches are complementary, and often both reaction types are consecutively used in the production of a single compound. Biocatalysis offers clear advantages, such as high chemo- or even enantioselectivity, and superior catalytic activity in mild, physiological conditions. In order to achieve such performance, biocatalysts often use catalytic centers and pathways that are not encountered in classical chemocatalysis. Additionally, the protein matrix surrounding a catalytic center has been optimized by the process of evolution to maximize catalyst performance, e.g., by positioning or concentration of the reaction substrates, or by creating local optima of acidobasicity or polarity. Bioinspired catalysis uses such concepts of supramolecular organization, borrowed from biocatalysis, in creating new synthetic catalysts. However, a main hurdle in the design of bioinspired catalysts may be the complex and costly organic preparation of ligands or cages mimicking the protein mantles of biocatalytic centers. Therefore, our laboratory has focused in the past decade on the preparation of hybrid catalysts by embedding inorganic or semiinorganic active centers in inorganic matrices [1–5]. Beyond providing immobilization of the active center, the matrix should provide the optimum physicochemical environment for the catalytic center. In order to speed up the screening process, we have selected as supports easily available materials with gradually tunable host characteristics, such as zeolites or layered double hydroxides. Moreover, these materials can be decorated with active centers by simple processes such as ion exchange or isomorphic substitution. In this way, we have created large libraries of composite catalysts for application in reactions of fine chemicals. In the present contribution, we present one of these composite materials, a layered double hydroxide exchanged with tungstate, which is active in oxidative bromination, and therefore is a mimic of haloperoxidase enzymes.

Vanadium-containing bromoperoxidases (VBPO) form a class of enzymes that catalyze the oxidative bromination and iodination of organic compounds with H_2O_2

$$\mathrm{Org{-}H} + \mathrm{X^-} + \mathrm{H_2O_2} + \mathrm{H^+} \rightarrow \mathrm{Org{-}X} + 2\mathrm{H_2O} \quad (\mathrm{X} = \mathrm{Br^-}\ \text{or}\ \mathrm{I^-}). \tag{1}$$

* Corresponding author.
E-mail address: pierre.jacobs@agr.kuleuven.ac.be (P.A. Jacobs).

0021-9517/03/$ – see front matter
doi:10.1016/S0021-9517(02)00066-0

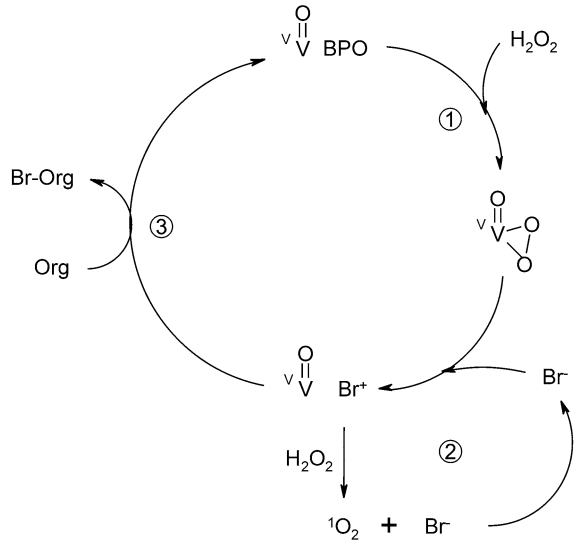

Fig. 1. Catalytic cycle for vanadium bromoperoxidase (VBPO) in contact with H_2O_2. Essential features are: **1.** peroxovanadate formation, **2.** bromide-assisted decomposition of H_2O_2 with $^1O_2$ formation, **3.** the bromination of organic compounds.

Numerous mechanistic studies have been performed to elucidate the catalytic cycle of the VBPO enzymes and three main features of bromoperoxidase activity have been recognized: (1) the formation of a peroxometal entity, (2) the bromide-assisted disproportionation of H_2O_2, and (3) the electrophilic bromination of organics (Fig. 1). The first step is the coordination of H_2O_2 to the V^V ion, producing a V^V-bound peroxide moiety [6]. The bromide reacts with the peroxide complex, yielding a free two-electron oxidized Br species. The primary oxidized species is presumably OBr^-; however, this is hard to establish due to rapid equilibration with hypobromous acid, bromine, and tribromide [7,8]. In a subsequent step, the intermediate Br^+ can either halogenate an appropriate organic substrate, or react with another equivalent of H_2O_2, forming dioxygen and water with regeneration of the bromide [9,10]. As O_2 originates from two-electron oxidation of H_2O_2 by Br^+, it is produced in the excited singlet state in accordance with spin conservation rules [11]. This bromide-assisted H_2O_2 decomposition differs from the classic well-known catalase reaction, in which H_2O_2 undergoes disproportionation, forming H_2O and ground-state O_2.

A number of synthetic peroxometal complexes have been tested as models of the peroxovanadium prosthetic group of VBPO. Such synthetic enzyme models are very helpful in studying the mechanistic details of biohalogenation chemistry and in understanding the factors that enhance the reactivity of peroxometal complexes toward halides. An extensive list of biomimics is given in Table 1 [12–20]. For the homogeneous VBPO mimics, appreciable catalytic activity is invariably observed in strong acid. However, if less acid is added, the activity is drastically lowered. In contrast, the VBPO enzymes operate optimally at nearly neutral pH (e.g., pH 6.5; see Ref. [8]).

The main challenge in VBPO mimicry is therefore to create a catalytic system featuring high activity, even of mild pH. In this respect, several groups have studied enzyme mimics in order to understand the relation between pH and catalytic activity. Several hypotheses have been proposed in the literature. First, differences in activity at various pH values may be explained in terms of the formation of various peroxo intermediates. Indeed, the coordination of H_2O_2 to the metal gives rise to an equilibrium mixture of peroxometal complexes, the composition of which is determined by the concentration of the acid [21–23]. Second, protons may facilitate the binding of H_2O_2 to the metal by labilizing oxo and hydroxo ligands [24]. Of course, this explanation only holds if the peroxometal formation is rate-determining. Finally, the solvent may play an important additional role, together with the proton concentration. Colpas et al. [25]

Table 1
Literature overview of synthetic catalysts mimicking VBPO activity

Catalyst	TOF[a]	H^+ concentration	Solvent	$[H_2O_2]$; $[Br^-]$	Ref.
VO_4^{3-}	15	0.05 M $HClO_4$	25% MeOH	5 mM; 0.43 M	[12]
V^VO–SB[b]	1.3[c]	Stoichiometric SB	DMF	4 mM; 0.1 M	[13]
V^VO–SB[b]	2.8	0.001 M $HClO_4$	DMF	4 mM; 0.1 M	[13]
K(18-crown-6)-$VO(O_2)$heida[b]	120	0.005 M triflic acid	Acetonitrile	5 mM; 15 mM	[14]
VO_4^{3-}	0.17	0.12 M $HClO_4$	$H_2O/CHCl_3$	20 mM; 0.05 M	[15,16]
MoO_4^{2-}	48	0.1 M $HClO_4$	25% MeOH	1.5 mM; 0.5 M	[17]
MoO_4^{2-}	1.8	10^{-5} M (acetate buffer)	25% MeOH	0.3 mM; 1 M	[16]
$MoO(O_2)_2(ox)^{2-}$	1.7[d]	10^{-5} M (oxalate buffer)	25% MeOH	—; 1 M	[17]
$MoO(O_2)_2(ox)^{2-}$	3.2	10^{-5} M (oxalate buffer)	Water	1 mM; 0.1 M	[18]
WO_4^{2-}	95	0.5 M $HClO_4$	Water	1 mM; 0.1 M	[17]
WO_4^{2-}	24	0.01 M $HClO_4$	25% MeOH	1 mM; 2 M	[17]
CH_3ReO_3	85	1 M $HClO_4$	Water	1 mM	[19]
Ti-MCM-48	0.16	3×10^{-7} M (hepes buffer)	Water	10 mM; 0.1 M	[20]

[a] TOF = mole Br^- oxidized per mole catalyst and per h.
[b] SB = schiff base; heida = *N*-(2-hydroxyethyl)iminodiacetate.
[c] In the absence of added acid, the reaction is not catalytic in the metal.
[d] Stoichiometric reaction. Only 1 mole of product per mole of metal is formed; hence $MoO(O_2)_2(ox)^{2-}$ is a reagent and not a catalyst.

found that the bromide oxidation activity of peroxovanadate complexes was higher in acetonitrile than in water. This was explained in terms of changes of the relative basicity of the active complex. In the nonprotic solvent, the active protonated V^V oxoperoxo complex is less dissociated than in water, and hence requires fewer H^+ ions for high activity. The same effect may be at the origin of the high activity of the enzymes, for which leveling of the pH may occur in the hydrophobic pockets in the protein interior [26].

A heterogeneous VBPO bioinspired catalyst has been reported, namely a Ti-containing silicate, Ti-MCM-48 [20]. Although this catalyst is active at neutral pH, the activity is rather modest. Recently, we reported the oxidative bromination of various unsaturated organic compounds over WO_4^{2-}-exchanged layered double hydroxides (LDHs). Extraordinarily high bromination activities were observed in comparison with many other homogeneous and heterogeneous oxidation catalysts even in benign reaction conditions [27–29]. In this report, we investigate in detail how the synthetic LDH catalyst imitates biohalogenation by vanadium bromoperoxidase VBPO. Experiments are therefore focused on the mechanistic aspects of bromination by LDH catalysts. Relationships are sought between the activity of the solid catalyst and its composition. Special attention is paid to the stability of the catalyst in terms of reusability and transition metal leaching during the oxidation process.

2. Experimental

2.1. Materials

All substrates and solvents were obtained from commercial sources in the highest grade available and were used without further purification.

2.2. Catalytic experiments

2.2.1. Phenol red and monochlorodimedone (MCD) bromination

The standard assay for bromoperoxidase activity is the bromination of phenol red or MCD. Spectral changes were followed with a UV–vis spectrophotometer in 2-mm path length quartz cuvettes. Data analysis was performed at 598 nm, the λ_{max} for bromophenol blue, or at 290 nm, the λ_{max} for MCD. Initial rates dA_{598}/dt and $-dA_{290}/dt$ were measured from the slope of the linear part of the absorbance vs time curve in order to obtain the oxidation rate of the bromide anions. For phenol red, this value is multiplied by 4 since four Br atoms are introduced into one phenol blue molecule. Activities were determined at room temperature, with 700 rpm stirring, using 0.05–0.5 mM metal catalyst, 1–5 mM H_2O_2, 0.1 M NH_4Br in 20 ml solvent (H_2O : MeOH : THF = 4 : 3 : 2), and 0.05 mM phenol red or MCD.

2.2.2. Bromination of DMT

Bromination of 2,3-dimethoxytoluene (DMT) with $FeBr_3$ and Br_2 in MeOH results exclusively in the ring-brominated DMT, whereas with Br_2 in CCl_4 the methyl group is also brominated. For 2,3-dimethoxybenzylbromide, the parent ions at $m/z = 232$ and 230 are very weak: 232 (1), 230 (1), 218 (1), 216 (1), 202 (3), 200 (3), 151 (10), 136 (40), 105 (19), 91 (50), 77 (32), 65 (100), 63 (53). At contrast, in the mass spectrum of ring-brominated dimethoxytoluene, the parent ions are the most abundant species: 232 (100), 230 (100), 217 (46), 215 (46), 189 (19), 187 (19), 121 (11), 108 (76), 93 (60), 77 (38), 65 (41), 63 (44).

Bromination of DMT is conducted at ambient temperature (700 rpm) for 125 min using 0.75 mM metal on LDH, 33 mM DMT, 0.33 M NH_4Br, and 55 mM H_2O_2 (final concentration) in a water–methanol (50 : 50) mixture. The H_2O_2 is added in five portions equally divided over the reaction time.

2.2.3. Detection of $^1O_2$ chemiluminescence

The formation of singlet dioxygen was monitored by the chemiluminescence from the spin-forbidden transition ($^1\Delta_g \rightarrow {}^3\Sigma_g^-$) at 1270 cm^{-1} using a liquid-N_2-cooled Ge detector. Reactions were performed in a cuvette (1 × 1 × 4 cm) and were started by adding 100 mM H_2O_2 into a stirred suspension containing 20 mg solid catalyst and 0.1 M NH_4Br in 3 ml D_2O–CD_3OD. Reactions were repeated in the absence of the bromide source and in the presence of 55 mM monochlorodimedone. The NIR spectra were recorded continuously between 1220 and 1350 nm at 1 nm/2.2 s. For each sample, 10 scans were accumulated. As a reference, $^1O_2$ was generated photochemically with the sensitizer $Ru(bpy)_3^{2+}$.

2.3. Instrumentation

Identification and quantification of reaction products were performed with GC (HP 5890 gas chromatograph with a 50-m Chrompack CP-Sil 5 column, equipped with FID) and were based on retention times and suitable response factors, respectively. In order to confirm the identity of the products, GC-MS was performed with a Fisons system equipped with a 50-m CP Sil-5 column. Bromination of phenol red or monochlorodimedone was followed using a Perkin–Elmer Lambda 12 spectrophotometer. Identification of the bromophenol blue was performed by liquid ^1H NMR on a Bruker AMX-300 instrument (300 MHz).

2.4. Synthesis and characterization of the catalysts

2.4.1. Preparation of LDH precursor

All LDHs are prepared by co-precipitation at 298 K and constant pH according to procedures described in detail elsewhere [30,31]. For the MgAl–NO_3^-, for instance, the pH of 100 ml deionized and boiled water in a 1 liter three-neck round-bottom flask was adjusted to 10 ± 0.2 by 1 N

NaOH, followed by the simultaneous addition of 120 ml of 0.3 M $Al(NO_3)_3 \cdot 9H_2O$ and 120 ml of 0.7 M $Mg(NO_3)_2 \cdot 6H_2O$ (60 ml/h) under N_2 atmosphere at room temperature. The pH of the slurry was maintained at 10 ± 0.2 by addition of 1 N NaOH. Upon complete addition of the NO_3^- salts, the suspension was stirred for 24 h at ambient temperature. The white precipitate was washed and centrifuged four times and was dried by lyophilization (yield $\sim$ 90% on a weight basis). For Zn- and Ni-containing LDHs, the pH of precipitation was kept at 8–8.5. The synthesis of a Br^--containing MgAl–LDH was performed starting from the Mg and Al nitrate salts, in a large excess (2 M) of NaBr.

2.4.2. Preparation of the metal-anion-exchanged LDHs

Generally, 1.5 g of the LDH precursor is contacted with an aqueous solution of 1.875 mM of, e.g., Na_2WO_4 (150 ml) and stirred over a period of at least 12 h at ambient temperature under N_2 atmosphere. The eventual solid products (e.g., LDH–WO_4^{2-}) were obtained by repeated centrifugation–washing cycles and by lyophilization. The final catalysts contain approximately 0.18 mmol metal (W or Mo) for one gram of solid material. In the case of vanadate, the exchange solution contained 3.75 mM $NaVO_3$, and hence, the ultimate V content in the final catalyst was somewhat higher (~ 0.31 mmol V g^{-1}). All the preparative procedures on LDHs were performed with deionized and boiled water, which was cooled under nitrogen in order to preclude contamination by CO_2.

The decavanadate-exchanged LDH was synthesized according to literature procedure [32–34]. After the rehydration of 1 g LDH precursor in 100 ml water at room temperature, the pH of the suspension is quickly brought at 4.5 with 2 M HNO_3. In another recipient, 1 g $NaVO_3$ is solubilized in 33 ml hot water and acidified at pH 4.5, giving an orange solution of decavanadate species. The colored solution is added to the LDH suspension over 15 min at room temperature, while keeping the pH at 4.5. After 4 h of stirring, the suspension is centrifuged and washed several times, yielding a yellow–orange solid.

2.4.3. Preparation of Ti-zeolites and zeolite-encapsulated complexes

Zeolite-entrapped bipyridine complexes were prepared as previously described, starting with partial exchange of NaY zeolites with Mn^{2+} and Fe^{2+} from $Mn(OAc)_2 \cdot 4H_2O$ and $FeSO_4 \cdot 7H_2O$, respectively [35]. After dehydration of the exchanged zeolite at 423 K, a twofold excess of crystalline bipyridine with respect to the metal ion was mixed with the dry zeolite. Heating for 24 h at 363 K then results in intrazeolite chelation, and after Soxhlet extraction to remove free ligand, the $Mn(bpy)_2Y$ and $Fe(bpy)_2Y$ catalysts are obtained. TS-1 and Ti,Al-Beta were prepared according to well-known literature procedures [36,37]; for Ti-MCM-41, the recipe using grafting of $TiCp_2Cl_2$ onto a preformed MCM-41 matrix was followed [38].

2.4.4. Physical measurements

The crystallinity and the basal spacing were controlled by X-ray powder diffraction (XRD) using a Siemens D5000*matic* diffractometer, equipped with a Ni-filtered Cu-K_α radiation of 1.5418 Å at 40 kV and 50 mA. The diffractograms were recorded between $2\theta = 3°$ and $2\theta = 65°$ with a scanning rate of 1° per minute. The infrared spectra (IR) were obtained from pressed KBr pellets in a Nicolet FT-IR 730 spectrophotometer. The IR spectra (200 scans) were recorded between 400 and 4000 cm^{-1}. FT-Raman spectra were collected on a Bruker IFS200, with 1062-nm excitation and 50 mW laser power. Intermediate peroxotungstate species on the LDH were observed with diffuse reflectance spectroscopy (DRS) on a Varian Cary05 UV–vis–NIR spectrophotometer, equipped with an integrating sphere accessory. The measurements were performed on the solid LDH–WO_4^{2-} sample before and after addition of H_2O_2. $BaSO_4$ was used to obtain the baseline.

3. Results and discussion

3.1. Catalyst characterization

XRD patterns of as-synthesized LDH materials gave evidence for high phase purity. The unit cell parameters were calculated from the d_{006} and d_{009} reflections, for c_0, and from d_{110}, for the a_0 parameter [30,31]. As can be seen in Table 2, the values slightly vary with the size of the octahedrally coordinated ions in the layer structure and with the nature of the charge compensating anion, viz. Cl^-, NO_3^-, and Br^-. The X-ray patterns hardly change upon exchange of WO_4^{2-}, MoO_4^{2-}, and VO_3^-, which indicates that at the low exchange levels used, there is no appreciable intercalation of these oxyanions. In contrast, pillaring of the structure was observed when MgAl–LDH was exchanged with an excess of decavanadate at pH 4.5 (Table 2) [34].

The presence and the nature of the exchanged oxyanions were confirmed with vibrational spectroscopy. Thus, IR and particularly Raman make it possible to identify the exchanged tungsten and molybdenum anions as monomeric WO_4^{2-} and MoO_4^{2-}, respectively [31]; V is present as

Table 2
Unit cell parameters of synthesized LDH structures, as calculated from X-ray diffraction patterns[a]

Support	c_0 (Å)	a_0 (Å)
MgAl(2.3)–Cl^-	23.66	3.05
MgAl(2.3)–NO_3^-	24.52	3.07
MgAl(2.3)–Br^-, NO_3^-	25.17	3.08
ZnAl(2.3)–Cl^-	23.48	3.06
ZnAl(2.3)–NO_3^-	26.52	3.08
NiAl(2.9)–Cl^-	23.40	3.03
MgAl(2.3)–$V_{10}O_{28}^{6-}$	35.4	3.04

[a] Numbers in parentheses indicate the elemental ratio of the two cations in the octahedral layers.

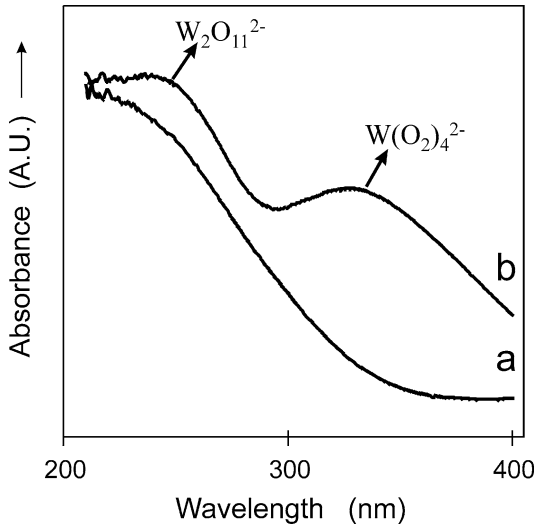

Fig. 2. Influence of H_2O_2 on the UV–vis DR spectrum of LDH–WO_4^{2-}, before (a) and after (b) addition of H_2O_2.

cyclic species $(VO_3)_n^{n-}$ ($n \geqslant 3$) when it is exchanged without any pH correction on MgAl–LDH; and the decavanadate structure is intact after incorporation into a pillared LDH material [34].

3.2. Evidence for a bromoperoxidase-like catalytic cycle

In following experiments, it is checked whether the LDH-based catalysts display the aforementioned diagnostic characteristics of the enzymatic pathway of bromoperoxidases. Tungstate exchanged on MgAl–NO_3^- or MgAl–Cl^- precursors, denoted as MgAl–WO_4^{2-}, was used as model catalyst in all experiments.

3.2.1. Formation of the peroxotungstates

Evidence for the reaction of H_2O_2 with the immobilized tungstate is obtained from diffuse reflectance spectroscopy (Fig. 2). Upon addition of H_2O_2, the white MgAl–WO_4^{2-} solid rapidly turns slightly yellow. In the UV–vis spectrum two broad bands appear at 235 and 330 nm. By analogy with the literature, the band at 235 nm is assigned to the $O_2^{2-} \rightarrow$ W charge transfer transition of a diperoxotungstate (e.g., $WO_2(O_2)_2^{2-}$, $W_2O_3(O_2)_4^{2-}$), whereas the band at 330 nm is ascribed to the $O_2^{2-} \rightarrow$ W charge transfer in the tetraperoxotungstate $W(O_2)_4^{2-}$ [39–41]. So, in analogy to the active V site in the enzyme, tungstate is transformed into its peroxo forms upon exposure of the solid MgAl–WO_4^{2-} to H_2O_2.

3.2.2. Evidence for oxidative bromination of organic compounds

The conversion of the dye phenol red (phenolsulfonephthalein) into bromophenol blue (tetrabromophenolsulfonephthalein) is a common test to monitor bromination activity under peroxidative conditions:

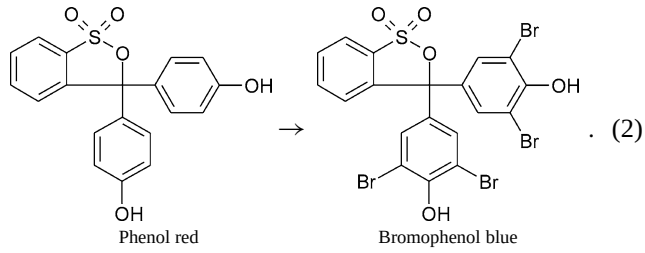

(2)

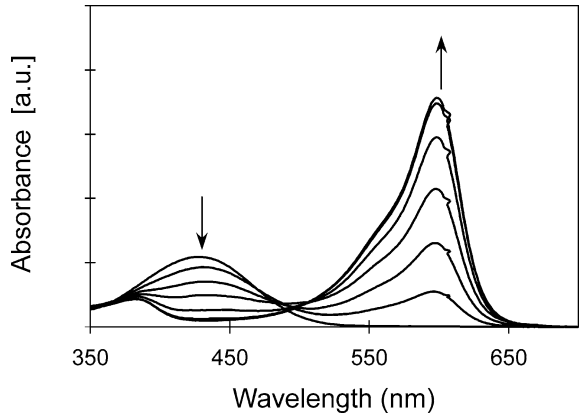

Fig. 3. Oxidative bromination of phenol red catalyzed by LDH–WO_4^{2-}: 2.5 mg MgAl–WO_4^{2-}, 0.1 M NH_4Br, 2.5 mM H_2O_2, 0.2 mM phenol red. The solid catalyst was removed before monitoring each UV–vis spectrum; sampling every 10 min.

The widespread use of this dye stems from its ability to undergo rapid and stoichiometric bromination and from the ease with which this can be monitored using UV–vis spectroscopy [42,43]. When MgAl–WO_4^{2-} is allowed to react with phenol red in the presence of H_2O_2 and NH_4Br, the yellow color of the reaction mixture rapidly changes to deep-blue. Figure 3 shows the electronic absorption spectra collected during such a color change. From these spectra, the disappearance of phenol red ($\lambda_{max} = 429$ nm; $\varepsilon = 21.4\ mM^{-1}\,cm^{-1}$) and the formation of the blue compound ($\lambda_{max} = 598$ nm; $\varepsilon = 70.4\ mM^{-1}\,cm^{-1}$) are evident [42]. That bromophenol blue is indeed formed in the MgAl–WO_4^{2-}/Br^-/H_2O_2 reaction mixture is confirmed by ^{1}H NMR spectroscopy. For the purpose of product identification, a 250-ml scale experiment was performed. The violet-blue-colored compound was extracted with tetra-*n*-hexylammonium chloride into dichloromethane and the organic layer was evaporated to dryness. The ^{1}H NMR spectrum of the remaining blue solid shows one singlet (7.29, 4*H*), two doublets (7.01 and 7.90, 1*H* each, $J =$ 7.5 Hz), and two triplets (7.41 and 7.50, 1*H* each, $J =$ 7.5 Hz) (Fig. 4), which agrees with the resonances of authentic bromophenol blue [42].

In the absence of MgAl–WO_4^{2-}, and within the same time scale, no bromophenol blue is formed. This shows that MgAl–WO_4^{2-} is the catalyst for phenol bromination by H_2O_2 and Br^-. From the example in Fig. 3, the turnover rate of MgAl–WO_4^{2-} can be calculated as 8.5 moles of

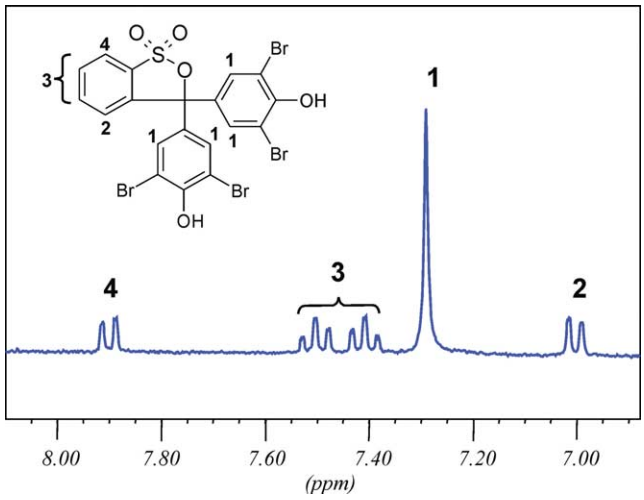

Fig. 4. ^{1}H NMR spectrum of the blue compound obtained from the LDH–WO_4^{2-}-catalyzed peroxidative bromination of phenol red, measured in DMSO-d_6.

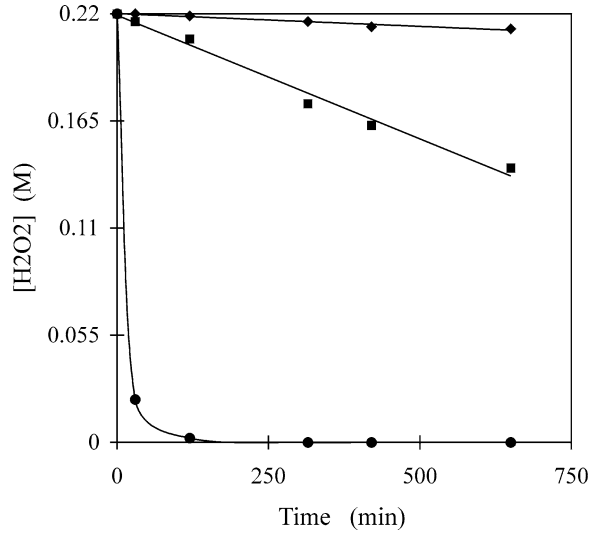

Fig. 5. Effect of charge-compensating co-anion on the decomposition of H_2O_2: 0.1 g solid LDH–WO_4^{2-}, 0.22 M H_2O_2, 20 ml MeOH. Anions on the support are NO_3^-(■) or Br^-(●). (♦) = blank with LDH–NO_3^- without WO_4^{2-}.

bromophenol per mol W and per h, in 2.5 mM H_2O_2 and at 298 K.

3.2.3. Evidence for the electrophilic nature of the brominating species

The bromination with the VBPO enzymes is an electrophilic process. The present MgAl–WO_4^{2-} catalyst forms similar active species, as demonstrated in an experiment with the probe molecule 2,3-dimethoxytoluene (DMT). This substrate can be used to distinguish between electrophilic and radical bromination [44]

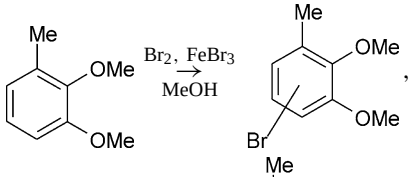

(3)

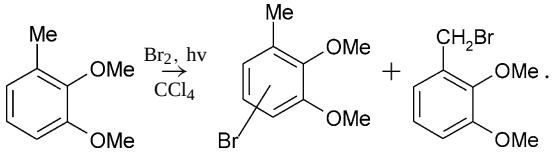

(4)

When 80 mg MgAl–WO_4^{2-} is stirred at room temperature in 20 ml of aqueous methanol containing NH_4Br (0.3 M), DMT (0.03 M), and H_2O_2 (0.05 M), ring-substituted bromo-DMT is formed exclusively at DMT conversion of 24%. This points to an electrophilic bromination mechanism (Eq. (3)), since for radical processes dimethoxybenzylbromide would also be formed (Eq. (4)). The active bromide intermediate can therefore be denoted as Br^+ rather than Br*.

3.2.4. Evidence for the Br-assisted H_2O_2 decomposition

As stated above, a haloperoxidase assisted by Br^- anions catalyzes the decomposition of H_2O_2 into singlet oxygen ($^1O_2$) in the absence of any organic substrate. An analogous effect of bromide anions on the decomposition of H_2O_2 is observed with the MgAl–WO_4^{2-} catalyst. Figure 5, for instance, shows the consumption of H_2O_2 when 0.1 g of MgAl–WO_4^{2-} (0.94 mM WO_4^{2-}) containing Br^- or NO_3^- as compensating anions is added to 0.22 M H_2O_2 in MeOH. The H_2O_2 decomposition rates for the various catalysts are 2.1×10^{-6} mol l^{-1} h^{-1} for the material with NO_3^- charge compensation, vs 1.3×10^{-4} mol l^{-1} h^{-1} for the Br^--containing catalyst. From the data, it is clear that the bromide anion promotes the disappearance of H_2O_2.

The slow H_2O_2 decomposition with the NO_3^- compensating anion is due to the thermal instability of the peroxotungstates and the formation of $^1O_2$, in analogy with the peroxomolybdates [45,46]. However, in the presence of Br^-, the decomposition of H_2O_2 proceeds more than 60 times faster. Hence, bromide anions and WO_4^{2-} jointly catalyze the decomposition of H_2O_2 in O_2 and water

$$Br^- + H_2O_2 \xrightarrow{WO_4^{2-}} Br^+ + 2OH^-,$$
$$Br^+ + H_2O_2 + 2OH^- \longrightarrow Br + {}^1O_2 + 2H_2O. \quad (5)$$

The electronic state of the produced O_2 is investigated by monitoring the chemiluminescence in the near-infrared region using a Ge detector [47–49]. The results of the luminescence measurements performed on mixtures containing a MgAl–WO_4^{2-} catalyst, H_2O_2 and Br^- are summarized in Fig. 6. Deuterated solvents were used since the lifetime of singlet dioxygen is much longer in a deuterated medium than in protonated solvents. Figure 6a shows the typical $^1O_2$ emission observed near 1269 nm when H_2O_2 is added to MgAl–WO_4^{2-} and NH_4Br in a deuterated solvent. If the bromide source is omitted from the reaction, no emission is detected (Fig. 6b). These two observations clearly demonstrate the assistance of the bromide anions in the production of $^1O_2$.

To investigate whether $^1O_2$ formation and bromination result from the same intermediate, as postulated for the

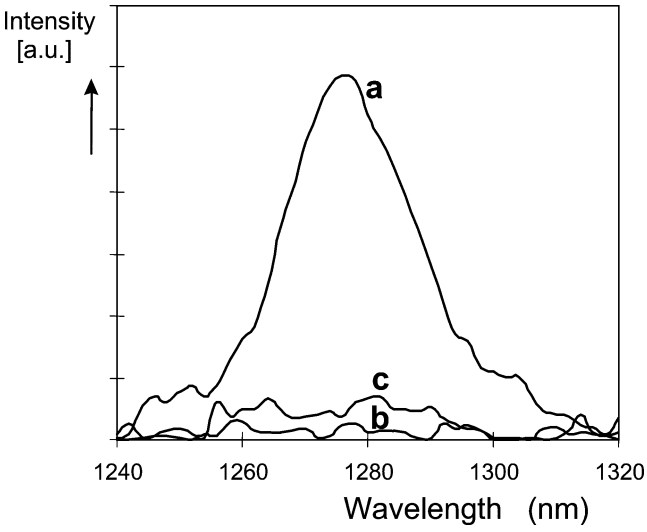

Fig. 6. Near-IR luminescence of $^1O_2$ at 1269 nm. 100 mM H_2O_2, 20 mg WO_4^{2-}-exchanged LDH–NO_3^- in 3 ml deuterated solvent (D_2O : MeOH = 3 : 1): (a) 0.1 M NH_4Br; (b) no NH_4Br; (c) 0.1 M NH_4Br and 55 mM monochlorodimedone.

enzyme (see cycle in Fig. 1), the chemiluminescence was monitored in presence of monochlorodimedone (MCD). This model substrate can easily be brominated and is commonly used, together with phenol red, to determine bromoperoxidase activity (8):

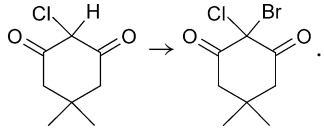

(6)

As can be seen from Fig. 6c, MCD addition causes a drop in the luminescence intensity to 6–7% of the original value, indicating that MCD bromination competes with $^1O_2$ formation. In addition, UV–vis spectroscopy of the supernatant shows that this drop in accompanied by the formation of 2-Br-2-Cl-1,3-cyclohexanedione. The formation of the latter was derived from the decrease of the absorbance at 290 nm, as a consequence of the 200 times smaller molar extinction coefficient of the bromination product in comparison with that of MCD (data not shown).

3.3. Activity and stability of the bioinspired catalyst

In this section, the effect of the immobilization of a transition metal anion (e.g., WO_4^{2-} on LDH) on its bromination activity is investigated. In order to find the conditions for maximum activity, parameters of catalyst composition and of reaction conditions, e.g., H_2O_2 concentration, are investigated. The activity of the LDH supported catalysts is also compared with various heterogeneous redox systems and with an immobilized enzyme. Finally, the stability of the LDH-supported catalyst is discussed based on catalyst regeneration and leaching experiments.

Bromoperoxidase activities were determined using extremely reactive substrates. This ensures that, at least in the initial stage of the reaction, all the oxidized Br species react with the substrate rather than with H_2O_2, which would lead to $^1O_2$. Indeed, most of the kinetic profiles of substrate disappearance vs time were essentially linear, i.e., zero order, except near the end of the reaction due to reagent depletion. Appropriate probe substrates are phenol red and MCD. In order to compare activities of catalysts, the following reaction parameters are defined:

Bromination rate (ν_{Br})

$$\nu_{Br} = \frac{\text{moles Br}^- \text{ oxidized}}{\text{time} \cdot \text{volume}} \tag{7}$$

Turnover frequency (TOF)

$$\text{TOF} = \frac{\text{moles Br}^- \text{ oxidized}}{\text{moles exchanged metal} \cdot \text{time}} \tag{8}$$

Specific activity (SA)

$$\text{SA} = \frac{\text{moles Br}^- \text{ oxidized}}{\text{total weight of oxyanion exchanged LDH} \cdot \text{time}} \tag{9}$$

3.3.1. Homogeneous versus heterogeneous catalysis

Bromination of phenol red is carried out in homogeneous conditions with the d^0 transition metal anions VO_3^-, WO_4^{2-}, and MoO_4^{2-}, and with the same anions including decavanadate immobilized on a MgAl–NO_3^- LDH via anion exchange. The results of the reactions are listed in Table 3.

The VO_3^-, MoO_4^{2-}, and WO_4^{2-} catalysts exhibit a much higher activity in an LDH environment than in solution, even on a total catalyst weight basis (compare ν_{Br} and SA for entries 2 and 6, 3 and 8, and 4 and 9). For bromination of phenol red under identical reaction conditions, the turnover rate TOF of MoO_4^{2-} is enhanced more than 400 times by immobilization on the positively

Table 3
Catalytic bromination of phenol red with homogeneous and LDH-immobilized catalysts[a]

Entry	Catalyst	$\nu_{Br} \times 10^6$ (mmol $l^{-1}\,s^{-1}$)	TOF (h^{-1})	SA (mmol $g^{-1}\,h^{-1}$)
1	–	0.01	–	–
2	NH_4VO_3	0.02	0.001	0.015
3	Na_2MoO_4	0.67	0.050	0.3
4	Na_2WO_4	3.9	0.280	1.1
5	MgAl–LDH	2.0	–	0.03
6	MgAl–VO_3^-	6.0	0.100	0.04
7	MgAl–$V_{10}O_{28}^{6-}$	0.8	0.013	0.004
8	MgAl–MoO_4^{2-}	280	20.100	3.7
9	MgAl–WO_4^{2-}	300	21.600	4.0

[a] Reaction conditions: catalysts: 0.05 mM soluble catalyst; 2.7 mg MgAl–NO_3^-; 2.7 mg LDH–MO_4^{2-} (from the MgAl–NO_3^- precursor) containing 0.05 mM W or Mo; 5.4 mg MgAl–VO_3^- (or 0.2 mM V); or 6.0 mg MgAl–$V_{10}O_{28}^{6-}$ (or 2 mM V). Other conditions: 2.5 mM H_2O_2, 0.05 mM phenol red, 0.1 M NH_4Br, 10 ml H_2O : MeOH : THF (4 : 3 : 2), 293 K.

charged LDH structure. In absence of a catalyst, the reaction produces 0.01 μM bromophenol blue per h, whereas with the LDH–WO_4^{2-} catalyst, the rate is 0.27 mM h^{-1}, or 27,000 times faster (entries 1 and 9). This strongly increased activity in mild pH conditions ($6 < -\log[H^+] < 8$) is in sharp contrast with previous, homogeneous mimics, which generally require strong acid ($-\log[H^+] < 2.5$) to achieve comparable catalytic activities (see Table 1).

Conceptually, the high activity of the LDH–WO_4^{2-} mimic is likely due to its unique supramolecular architecture. The large positive electric potential of the LDH–WO_4^{2-} surface induces an enrichment of bromide anions close to the surface. Moreover, the simultaneous presence of bromide and peroxotungstate anions (e.g., $W_2O_3(O_2)_4^{2-}$ and $W(O_2)_4^{2-}$) on the catalyst surface decreases the electrostatic repulsion between these negatively charged reaction partners. This architectural aspect, namely spatial organisation of the reaction partners, and electrical shielding, is totally lacking in the presently known homogeneous VBPO mimics. Note that charge shielding at the active site is also important for enzymes, and has recently been documented for natural VBPO. For instance, for the VBPO of *Curvularia inaequalis*, the negative charge of the peroxovanadate is compensated by the surrounding Arg, His, and Lys residues [26].

A rather low activity is found for decavanadate, supported in an LDH structure (Table 3, entry 7). Such low TOFs can indeed be expected, since only one or a few V atoms in a $V_{10}O_{28}^{6-}$ anion can interact with H_2O_2. Moreover, the XRD analysis shows that the LDH structure is truly intercalated with decavanadate anions, which means that many of these are located in the interlayer galleries, and hence are rather inaccessible for the substrates H_2O_2 and Br^-.

3.3.2. Influence of the composition of the LDHs

To investigate the influence of the support composition on the bromination activity, various LDH supports were exchanged with the same amount of WO_4^{2-} and tested in the oxidative bromination of phenol red and MCD (Table 4). Note that the activity measured when MCD is used is systematically higher than that when phenol red is used. This may be due to the higher H_2O_2 concentration used in combination with MCD, as will be explained later. Irrespective of the Br^+ trapping agent used, the following activity order was observed for the Cl^- containing supports: $Mg^{2+} > Ni^{2+} > Zn^{2+}$ (entries 1, 4, and 6). A similar order is obtained for the supports having NO_3^- as compensating anion: $Mg^{2+} > Zn^{2+}$ (entries 2 and 5). In contrast, there is no direct correlation of the activity with the exchanged co-anion. Whereas the Cl^- containing catalyst is more active than its NO_3^- analogue in the case of the MgAl supports, the reverse order is obtained for the ZnAl–LDHs (compare entries 1 and 2 with 4 and 5). Only a careful characterization of the supports will unequivocally explain these activity differences. At this point, it is assumed that the surface area and the electrical potential of the solid, which is associated with the nature of the anions and the total AEC, are likely to be key parameters. Anyhow, from this preliminary study, MgAl–Cl^-, MgAl–NO_3^-, and NiAl–Cl^- appear to be the three most preferred supports.

Table 4
Catalytic bromination of phenol red[a] and MCD[b] with WO_4^{2-} exchanged on various LDH supports

Entry	Support	TOF (h^{-1})
1	MgAl(2.3)–Cl^-	32.0[a], 70.6[b]
2	MgAl(2.3)–NO_3^-	21.6[a], 40.9[b]
3	MgAl(2.3)–Br^-, NO_3^-	6.2[a], 14.9[b]
4	ZnAl(2.3)–Cl^-	3.2[a]
5	ZnAl(2.3)–NO_3^-	6.8[a]
6	NiAl(2.9)–Cl^-	12.6[a]

[a] Reaction conditions: 2.7 mg LDH–WO_4^{2-} (or 0.05 mM W), 2.5 mM H_2O_2.

[b] 5 mM H_2O_2, 0.05 mM phenol red, 0.1 M NH_4Br, 10 ml H_2O : MeOH : THF (4 : 3 : 2).

3.3.3. Influence of the H_2O_2 concentration

Figure 7 depicts the effect of the H_2O_2 concentration on the bromination rate of phenol red with LDH–WO_4^{2-}. As can be seen, increasing the concentration of H_2O_2 brings along an increase of the bromination rate. For the enzymatic reaction, the bromination activity normally reaches an optimum at H_2O_2 concentrations of ca. 1–4 mM [50]. Higher concentrations are undesired, as they destroy the enzyme. In contrast, the rate of phenol red bromination by the LDH–WO_4^{2-} bioinspired catalyst is not saturated at H_2O_2 concentrations up to 10 mM. In practice, this means that the required H_2O_2 does not need to be added in small amounts, which opens perspectives for synthetic applications.

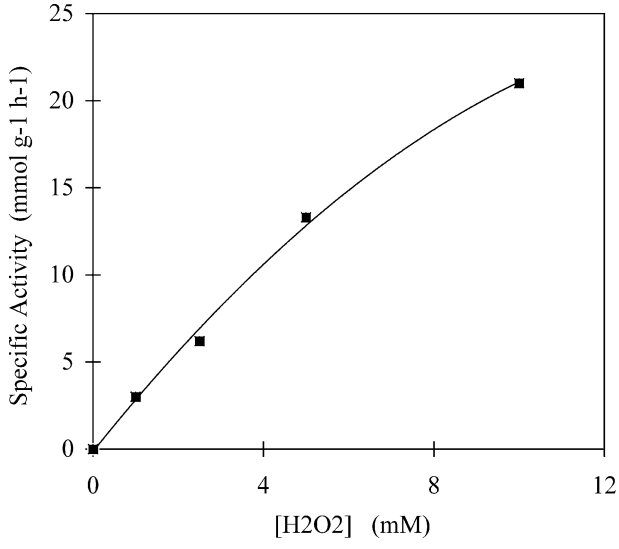

Fig. 7. Influence of the initial hydrogen peroxide concentration on the specific activity of WO_4^{2-}, exchanged on LDH–Cl^-, as obtained in the bromination of phenol red. Reaction conditions as in Table 4 except for the concentration of H_2O_2.

3.3.4. Comparison with heterogeneous catalysts and VBPO enzymes

Table 5 compares the activities of a soluble and an immobilized commercial bromoperoxidase and of several established heterogeneous redox catalysts and solid VBPO mimics with that of the LDHs. Ti-MCM-41 and Ti-MCM-48 contained 4 and 5 wt% Ti; TS-1 and Ti,Al-Beta had Ti content of 3.5 and 5 wt% Ti, respectively. The commercial VBPO is a lyophilized protein mixture (10% pure) extracted from C*orallina officinalis* (Sigma).

It is clear that WO_4^{2-} exchanged on MgAl–Cl^- is a much more active material than any other solid inorganic VBPO mimic, e.g., mesoporous Ti catalysts or any heterogeneous redox catalyst (Table 5, entry 5 vs entries 1–4). Amazingly, LDH–WO_4^{2-} turns out to be 700 times more active than Ti-MCM-48, which has recently been reported as an effective solid biomimic of VBPO [20]. If the two catalysts are compared in exactly the same reaction conditions (room temperature, 0.1 M KBr, 10 mM metal, 0.2 mM phenol red, pH = 6.5, and 10 mM H_2O_2 in H_2O as solvent; see Ref. [15], Fig. 1), the reaction is complete with LDH–WO_4^{2-} within 10–15 s, whereas with the Ti-MCM-48, the reaction lasts 137 min, and is at least 500 times slower.

Finally, while the use of V bromoperoxidase results in high activities (entry 8), immobilization of the enzyme is preferred in industrial applications to improve reusability and stability at elevated temperatures or high H_2O_2 concentrations. However, enzyme immobilization in general causes at least a 100-fold reduction of the activity per catalyst weight [51,52], which may be ascribed to reduced activity of the enzyme, but which is mainly the result of the additional weight of the support. For haloperoxidases in particular, activity reduction between 10^3 and 10^4 times upon immobilization has been reported [50,53]. Therefore, the LDH–WO_4^{2-} mimic presents an attractive alternative to the VBPO enzymes for practical use.

3.3.5. Heterogeneity and stability

In order to check the stability of the LDH–WO_4^{2-} catalyst, the same catalyst was reused during several consecutive reaction cycles. After completion of the reaction, the catalyst was separated from the reaction mixture by centrifugation and washed with the solvent mixture; then the next run was performed (Table 6). The results with the recycled catalyst invariably show unaltered activity, suggesting that LDH–WO_4^{2-} is a stable, heterogeneous catalyst. In this respect, it is important to stress that the LDH–WO_4^{2-} catalyst, in contrast to enzymes, is not sensitive to oxidative destruction, as a consequence of its completely inorganic structure.

Table 6
Comparison of the TOF (h^{-1}) of LDH–WO_4^{2-} before and after reuse of the catalyst[a]

	Run 1	Run 2	Run 3
LDH–WO_4^{2-}	21.6	20.2	20.8

[a] Conditions: as in Table 4.

Additional evidence for the retention of WO_4^{2-} on the LDH support is obtained from leaching experiments. In this experiment, the supernatant of vigorously stirred aqueous mixtures containing LDH–WO_4^{2-} and Br^- anions was analyzed for the presence of dissolved W. The results of Table 7 show that WO_4^{2-} anions remain fairly well retained after 24 h of stirring, even when the Br/W atomic ratio is as high as 1250. Not only WO_4^{2-}, but also its peroxo analogues show a higher affinity for the LDH–support than the bromide anions in the reaction conditions. Indeed, even in the presence of 30 mM H_2O_2, the degree of leaching of W in solution was less than 0.2 ppm, i.e., less than 0.3% of the total amount of W. Both the heterogeneity of tungstate and the constant catalyst activity are essential requirements for practical implementation.

4. Conclusion

Based on the information gained from spectroscopic and catalytic studies, it is clear that the catalytic cycle of LDH–WO_4^{2-} bears all essential characteristics of bromoperoxidase activity. Hence, a catalytic cycle similar to that for VBPO can be drawn, in which the V^VO and the $V^VO(O_2)$ groups are replaced by WO_4^{2-} and peroxotungstates respectively (Fig. 1). The activity of the bioinspired LDH–WO_4^{2-}

Table 5
Bromination of phenol red with heterogeneous catalysts and VBPO enzymes[a]

Entry	Catalyst	$[H_2O_2]$ (mM)	[metal] (mM)	TOF (h^{-1})	SA ($mmol\,g^{-1}\,h^{-1}$)
1	TS-1	2.5	0.5	0.001	0.00025
2	Ti,Al-β	2.5	0.3	0.051	0.016
3	Ti-MCM-41	2.5	0.3	0.056	0.047
4	Ti-MCM-48 (Ref. [15])	10	2.5	0.160	0.16
5	WO_4^{2-} on MgAl–Cl^-	10	2.5	109.600	20.3
6	$Mn(bpy)_2$-Y	2.5	0.05	nd[b]	nd[b]
7	$Fe(bpy)_2$-Y	2.5	0.05	0.001	0.00078
8	VBPO (Sigma)	–	–	–	600
9	Immobilized VBPO	–	–	–	0.15×10^{-6}

[a] Reaction conditions (1–3; 5–7): 0.05 mM phenol red, 0.1 M NH_4Br, 10 ml H_2O : MeOH : THF (4 : 3 : 2).
[b] Nothing detected.

Table 7
Leaching experiments of W (%) in the absence of organic substrate[a]

	0.1 M NH_4Br	0.3 M NH_4Br	0.5 M NH_4Br
Without H_2O_2			
After 40 min	0.12	0.23	0.32
After 24 h	0.33	0.60	0.73
With H_2O_2			
After 20 min[b]	0.06	0.20	0.27

[a] Conditions: LDH–WO_4^{2-} (0.4 mM W) in H_2O with 0.1, 0.3, or 0.5 M NH_4Br, in absence or presence of 30 mM H_2O_2.

[b] At this time, the concentration of H_2O_2 is still sufficient to keep W in its peroxo state, as can be derived from the yellow color of the solid.

catalyst is superior to that of immobilized commercial enzymes, even at nearly neutral pH. In view of the succesfull leaching tests, and in view of the excellent stability of the catalyst to high H_2O_2 concentrations, oxidative bromination with LDH–WO_4^{2-} is a synthetic alternative to bromination reagents such as N-bromo compounds or to Br_2 itself, which always produces one Br^- ion per Br atom incorporated into aromatic molecules. At contrast, the route with H_2O_2, bromide anions, and LDH–WO_4^{2-} presents a 100% atom economy based on Br. Concepts such as supramolecular organization of reagents and charge shielding, which are common in enzymology, are the basis of the high bromide oxidation activity. LDH-derived catalysts similar to those discussed in the present paper have already been shown to be useful in olefin epoxidation with or without bromide assistance, in the catalytic generation of excited state singlet dioxygen, and in several other oxidative transformations [29]. This illustrates the promise of this approach for broad application to large classes of organic transformations.

Acknowledgments

BFS is indebted to FWO (Belgium) for a postdoctoral fellowship. This work is supported by the Federal Government of Belgium in the frame of an IAP project on supramolecular catalysis and the Flemish government (GOA program). Further support was provided by FWO projects G.0355.99 (for NMR spectroscopy) and G.0334.99 (for Raman spectroscopy).

References

[1] D.E. De Vos, M. Dams, B.F. Sels, P.A. Jacobs, Chem. Rev. (2002), in press.
[2] D.E. De Vos, B.E. Sels, B.E. Jacobs, Cattech. 6 (2002) 14.
[3] B.E. Sels, D.E. De Vos, P.A. Jacobs, Catal. Rev. 43 (2001) 443.
[4] D.E. De Vos, B.E. Sels, P.A. Jacobs, Adv. Catal. 46 (2002) 1.
[5] D.E. De Vos, P.A. Jacobs, Catal. Today 57 (2000) 105.
[6] M.G.M. Tromp, G. Olafsson, B.E. Krenn, R. Wever, Biochim. Biophys. Acta 1040 (1990) 192.
[7] M.C.R. Franssen, Catal. Today 22 (1994) 441.
[8] A. Butler, J.V. Walker, Chem. Rev. 93 (1993) 1937.
[9] A.M. Held, D.J. Halko, J.K. Hurst, J. Am. Chem. Soc. 100 (1987) 5732.
[10] H.S. Soedjak, A. Butler, Biochem. Biophys. Acta 1079 (1991) 1.
[11] A.U. Khan, M. Kasha, J. Am. Chem. Soc. 92 (1970) 3293.
[12] R.I. de la Rosa, M.J. Clague, A. Butler, J. Am. Chem. Soc. 114 (1992) 760.
[13] M.J. Clague, N.L. Keder, A. Butler, Inorg. Chem. 32 (1993) 4754.
[14] G.J. Colpas, B.J. Hamstra, J.W. Kampff, V.L. Pecoraro, J. Am. Chem. Soc. 116 (1994) 3627.
[15] V. Conte, F. DiFuria, S. Moro, Tetrahedron Lett. 35 (1994) 7429.
[16] M. Andersson, V. Conte, F. DiFuria, S. Moro, Tetrahedron 36 (1995) 2675.
[17] G.E. Meister, A. Butler, Inorg. Chem. 33 (1994) 3269.
[18] M.S. Reynolds, S.J. Morandi, J.W. Raebiger, S.P. Melican, S.P.E. Smith, Inorg. Chem. 33 (1994) 4977.
[19] J.H. Espenson, O. Pestovsky, P. Huston, S. Staudt, J. Am. Chem. Soc. 116 (1994) 2869.
[20] J.V. Walker, M. Morey, H. Carlsson, A. Davidson, G.D. Stucky, A. Butler, J. Am. Chem. Soc. 119 (1997) 6921.
[21] A.F. Ghiron, R.C. Thompson, Inorg. Chem. 27 (1988) 4766.
[22] A.F. Ghiron, R.C. Thompson, Inorg. Chem. 28 (1989) 3647.
[23] A.F. Ghiron, R.C. Thompson, Inorg. Chem. 29 (1990) 4457.
[24] B.J. Hamstra, G.J. Colpas, V.L. Pecoraro, Inorg. Chem. 37 (1998) 949.
[25] G.J. Colpas, B.J. Hamstra, J.W. Kampf, V.L. Pecoraro, J. Am. Chem. Soc. 118 (1996) 3469.
[26] A. Messerschmidt, R. Wever, Biochem. Proc. Natl. Acad. Sci. USA 93 (1996) 392.
[27] B. Sels, D. De Vos, M. Buntinx, F. Pierard, A. Kirsch-De Mesmaeker, P. Jacobs, Nature 400 (1999) 855.
[28] B. Sels, D. De Vos, P. Jacobs, J. Am. Chem. Soc. 123 (2001) 8350.
[29] D. De Vos, J. Wahlen, B. Sels, P. Jacobs, Synlett 3 (2002) 367.
[30] S. Miyata, Clays Clay Miner. 23 (1975) 369.
[31] B.F. Sels, D.E. De Vos, P.J. Grobet, F. Pierard, F. Kirsch-De Mesmaeker, P.A. Jacobs, J. Phys. Chem. B 103 (1999) 11114.
[32] E. Lopez-Salinas, Y. Ono, Bull. Chem. Soc. Jpn. 65 (1992) 2465.
[33] M. Ulibarri, F. Labajos, V. Rives, R. Trujillano, W. Kagunya, W. Jones, Inorg. Chem. 33 (1994) 2592.
[34] A.L. Villa, D.E. De Vos, F. Verpoort, B.F. Sels, P.A. Jacobs, J. Catal. 198 (2001) 223.
[35] P.-P. Knops-Gerrits, D.E. De Vos, F. Thibault-Starzyk, P.A. Jacobs, Nature 369 (1994) 543.
[36] J.A. Martens, Ph. Buskens, P.A. Jacobs, A. van der Pol, J.H.C. van Hooff, C. Ferrini, H.W. Kouwenhoven, P.J. Kooyman, H. van Bekkum, Appl. Catal. A 99 (1993) 71.
[37] A. Corma, M.A. Camblor, P. Esteve, A. Martinez, J. Pérez Pariente, J. Catal. 145 (1994) 151.
[38] T. Maschmeyer, F. Rey, J.M. Thomas, Nature 358 (1995) 159.
[39] A.J. Dedman, T.J. Lewis, D.H. Richards, J. Chem. Soc. (1963) 2456.
[40] W.P. Griffith, J. Chem. Soc. (1963) 5345.
[41] M.H. Dickmann, M.T. Pope, Chem. Rev. 94 (1994) 569.
[42] E. de Boer, H. Plat, M.G.M. Tromp, R. Wever, M.C.R. Franssen, H.C. van der Plas, E.M. Meijer, H.E. Schoemaker, Biotechnol. Bioeng. 30 (1987) 607.
[43] M.C.R. Franssen, H.C. van der Plas, Adv. Appl. Microbiol. 37 (1992) 41.
[44] K.P.C. Vollhardt, Organic Chemistry, Freeman, New York, 1987.
[45] B.F. Sels, D.E. De Vos, P.A. Jacobs, Tetrahedron Lett. 37 (1996) 8557.
[46] B.F. Sels, D.E. De Vos, P. Grobet, P.A. Jacobs, Chem. Eur. J. 7 (2001) 2547.
[47] J.R. Kanofsky, J. Am. Chem. Soc. 106 (1984) 4277.
[48] R.R. Everett, J.R. Kanofski, A. Butler, J. Biol. Chem. 265 (1990) 4908.
[49] F. van Laar, D. De Vos, D. Vanoppen, B. Sels, P. Jacobs, A. Del Guerzo, F. Pierard, A. Kirsch-De Mesmaeker, Chem. Commun. (1998) 267.
[50] S. Aoun, M. Baboulène, J. Mol. Catal. B 4 (1998) 101.
[51] T. Kadima, M. Pickard, Can. J. Microbiol. 36 (1989) 302.
[52] T. Kadima, M. Pickard, Appl. Environ. Microbiol. 56 (1990) 3473.
[53] N. Itoh, L.Y. Cheng, Y. Izumi, H. Yamada, J. Biotechnol. 5 (1987) 29.